Ferromagnetic resonance and magnetoelastic demodulation in thin active films with an uniaxial anisotropy

A. Klimov, Y. Ignatov, Nicolas Tiercelin, Vladimir Preobrazhensky, Philippe Pernod, S. Nikitov

Ferromagnetic resonance and magnetoelastic demodulation in thin active films with an uniaxial anisotropy

Cite as: J. Appl. Phys. **107**, 093916 (2010); https://doi.org/10.1063/1.3382911
Submitted: 29 January 2010 • Accepted: 09 March 2010 • Published Online: 07 May 2010

A. Klimov, Yu. Ignatov, N. Tiercelin, et al.

Ferromagnetic resonance and magnetoelastic demodulation in thin active films with an uniaxial anisotropy

A. Klimov,[1,2] Yu. Ignatov,[1,2,4,a)] N. Tiercelin,[1] V. Preobrazhensky,[1,3] P. Pernod,[1] and S. Nikitov[2,4]
[1]*Joint International Laboratory LEMAC—IEMN (CNRS UMR 8520), PRES Univ. Lille Nord de France, EC Lille, BP 48, 59652 Villeneuve d'Ascq Cedex, France*
[2]*V. A. Kotel'nikov Institute of Radioengineering and Electronics, 125009 Moscow, Russia*
[3]*Joint International Laboratory LEMAC—Wave Research Center, A.M.Prokhorov General Physics Institute RAS, 119991 Moscow, Russia*
[4]*Moscow Institute of Physics and Technology (State University), 141700 Dolgoprudny, Russia*

(Received 29 January 2010; accepted 9 March 2010; published online 7 May 2010)

The results of experimental and theoretical studies of ferromagnetic resonance (FMR) and magnetoelastic excitations near the spin reorientation transition (SRT) in an uniaxial $TbCo_2/FeCo$ layered nanostructure and a $La_{0.7}Sr_{0.3}MnO_3$ film are reported. Experimental dependences of the amplitude of the reflected microwave signal versus the external magnetic field strength are presented in comparison with the theoretical ones. An increase in FMR reflectivity in the vicinity of SRT is clearly demonstrated. Low frequency magnetoelastic excitation of flexural vibrations of the samples by means of modulated microwave electromagnetic field is observed experimentally using a laser beam deflection technique. The increase in amplitude of vibrations at modulation frequency under combined FMR and SRT conditions is observed in agreement with the theory. © *2010 American Institute of Physics*. [doi:10.1063/1.3382911]

I. INTRODUCTION

Uniaxial magnetostrictive films with an artificial spin reorientation transition (SRT) induced by external magnetic field are of great practical interest.[1–4] Rare earth intermetallic compositions like $TbCo_2/FeCo$ which are usually under consideration in this matter provide giant magnetostriction, large values of the electromechanical coupling factor and other favorable properties.[5,6] The magnetoelastic sensitivity of micromagnetomechanical systems (MMMS) can increase about two order of value near SRT in magnetostrictive multilayer nanostructures.[1,2,7] The area in the vicinity of SRT in magnets has a number of dynamic and nonlinear features.[8–11] In particular high efficiency of subharmonic excitation of elastic vibrations was observed in MMMS near SRT.[12] Strong magnetoelectric effect was also obtained near SRT in a composite $TbCo_2/FeCo/PzT$ and $TbCo_2/FeCo/AlN$ multilayers.[13–15]

Magnetoelastic demodulation of electromagnetic waves can also become efficient in giant magnetostriction nanostructures near SRT. This phenomenon is of interest for high frequency control of MMMS. For microwave demodulation one can expect the most preferable conditions when SRT is combined with ferromagnetic resonance (FMR) in a magnetostrictive film.

In the present paper we study FMR and magnetoelastic demodulation in the uniaxial $TbCo_2/FeCo$ nanostructure deposited on Si cantilever. The results are compared with the ones obtained on $La_{0.7}Sr_{0.3}MnO_4$ thin film grown on $NdGaO_3$ substrate. The latter rare earth manganitestrontium perovskite thin film was chosen for its low high frequency (HF) absorption and its significant magnetostriction coefficient at room temperature.[16,17] In both cases the technology provides uniaxial in plane magnetic anisotropy and clearly expressed SRT.[18,19] Creation of SRT in giant magnetostriction $TbCo_2/FeCo$ exchange coupled nanostructures was achieved technologically by means of rf deposition under a steady state external magnetic field, while creation of SRT in the $La_{0.7}Sr_{0.3}MnO_4$ perovskite films was achieved technologically by means of lattice mismatch of the film and the substrate.

The results of measurements of FMR lines and magnetic field dependencies of amplitudes of low frequency (LF) magnetoelastic vibrations in the samples under consideration are compared with calculations.

II. EXPERIMENTAL RESULTS

Experimentally observed excitation of LF elastic vibrations of the cantilevers due to magnetoelastic demodulation of microwave electromagnetic field at FMR frequency is presented in this part. The scheme of the experimental setup is shown in Fig. 1. A high frequency sinusoidal signal modulated by LF square signal was used to feed the sample by means of the microstrip line (ML). The first sample was made of 25 bilayers of $(TbCo_2/FeCo)$ composition, and thickness 10 nm, deposited by rf sputtering on Si substrate of 20 mm $\times$ 4 mm $\times$ 60 μm dimensions. The second $La_{0.7}Sr_{0.3}MnO_3$ film, of thickness 200 nm, was deposited by laser ablation on a (110) $NdGaO_3$ substrate of 10 mm $\times$ 5 mm $\times$ 500 μm size. According to Ref. 19, at this crystal orientation of substrate the perovskite film has an uniaxial anisotropy with [001] hard axis. The hard axis was perpendicular to the long side of the samples. Both samples were successively installed in the static bias field H of an electro-

a)Electronic mail: yury.ignatov@ec-lille.fr.

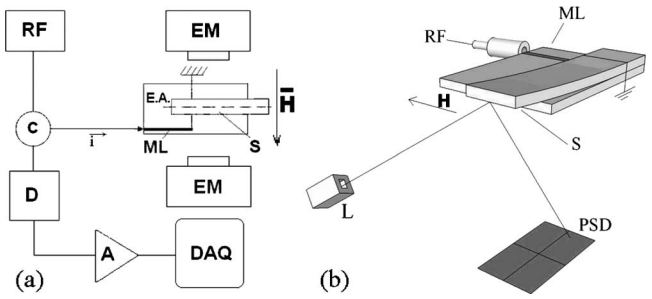

FIG. 1. Description of the experimental setup: (a)—HF excitation and measurement system: RF—radio frequency generator, C—circulator, EM—electromagnet, ML—microstrip line, E. A.—easy axis, S—sample, D— detector, A—amplifier, DAQ—data acquisition hardware ; (b)—optical system for the measurement of mechanical deflections: L—laser $\lambda=650$ nm, PSD—position sensitive detector).

magnet. Mechanical vibrations of the samples were observed optically by measurement of the deflection of a laser beam ($\lambda=650$ nm) using a position sensitive photodetector (PSD). Simultaneously, a part of the HF signal was split via the circulator C to the detector D, amplified by the lock-in amplifier and registered by the data acquisition (DAQ) block.

The value of the bias field, which induced SRT, was equal to 25 Oe for the $TbCo_2/FeCo$ nanostructure and 105 Oe for the $La_{0.7}Sr_{0.3}MnO_3$ perovskite film. Measured FMR curves are presented in Fig. 2 (solid lines). One can see that FMR amplitude is twice higher, when FMR conditions verge toward SRT [compare Figs. 2(a) and 2(b); Figs. 2(d) and 2(e)] and decreases sharply when FMR is far from SRT [Figs. 2(c) and 2(f)]. This phenomenon is caused by the increase in the magnetic susceptibility imaginary part.

The results of the optical detection of the flexural vibrations of the cantilever are presented in Fig. 3. One can see that the amplitude of the vibrations increases when FMR is excited near SRT. All results were observed at room temperature, when $La_{0.7}Sr_{0.3}MnO_3$ still has ferromagnetic order and a significant magnetoelastic coupling factor.[16,17]

In Figs. 2 and 3, only the frequency range over 800 MHz is presented. In the lower frequency range the experiment showed the dramatic decrease in FMR signal and vibration amplitude down to ten times (for the feeding frequency value 290 MHz) and more.

The attenuation coefficients of the mechanical vibrations of both samples were also measured. They were obtained by measurement of the relaxation time for the fundamental flexural mode assuming that the vibration amplitude was decaying exponentially. The obtained attenuation coefficients were $\delta=0.1\ s^{-1}$ for the $TbCo_2/FeCo$ nanostructure, and $\delta=0.25\ s^{-1}$ for the perovskite film.

III. THEORY AND DISCUSSION

The theory of LF elastic vibrations of the structure excited by LF electromagnetic field near SRT was already developed in Ref. 12. In the present paper, this approach is extended for LF elastic vibrations excited by modulated HF electromagnetic field. The mechanism of such a process is explained by the combined contributions of two nonlinearities: the nonlinearity of magnetostriction and the nonlinearity of magnetization dependence on the value of the alternative external magnetic field.

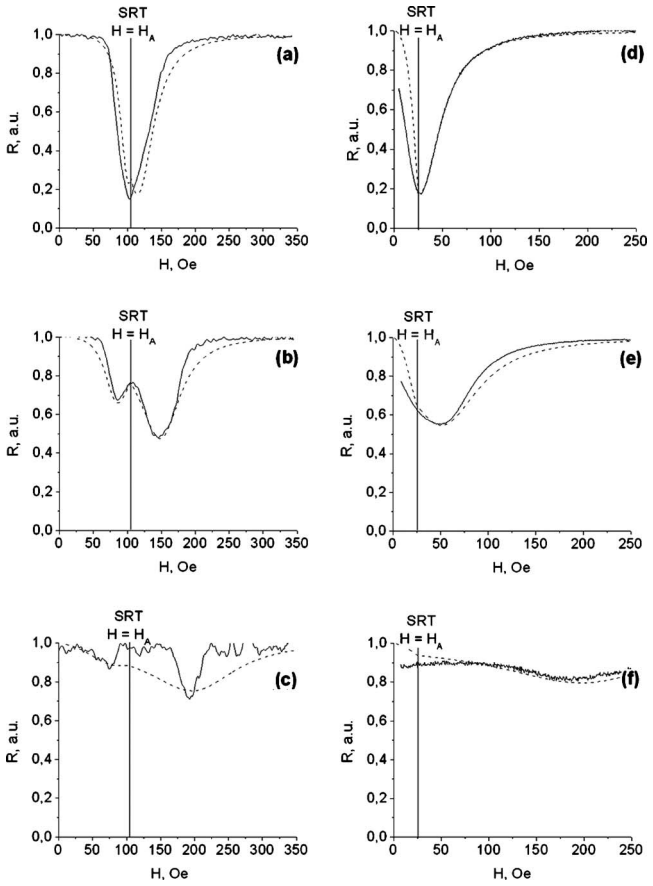

FIG. 2. Magnetic field dependence of the HF reflection coefficient R expressed in arbitrary units at different FMR frequencies for $La_{0.7}Sr_{0.3}MnO_3$ film [(a)—814 MHz, (b)—1183 MHz, (c)—1760 MHz] and for $TbCo_2/FeCo$ nanostructure [(d)—1172 MHz, (e)—2174 MHz, (f)—4918 MHz]: solid line-experiment, dashed line-theory.

The system geometry is presented in Fig. 4. We suppose that the thin film with magnetization $\vec{M}$ and thickness d_m is placed on a thick nonmagnetic substrate with thickness d. The easy axis of the film is along the length of the sample corresponding to the x-axis and perpendicular to the external magnetic field H applied along the y-axis. The magnetization $\vec{M}$ has the direction defined by the competition between the external magnetic field and the anisotropy.

Following the classical approach[20,21] one can derive the nonlinear equations of motion for magnetization and elastic strains by retaining high-order terms in the free energy. Overall energy of the sample consists of three parts: elastic F_e, magnetoelastic F_{me} and magnetic F_m ones.

$$F = F_e + F_{me} + F_m. \tag{1}$$

We assume that the structure is elastically isotropic. Thus the elastic part of energy volume density can be written in the following form:[22]

$$F_e^V = \tfrac{1}{2}C_{11}(u_{xx}^2 + u_{yy}^2 + u_{zz}^2) + C_{12}(u_{xx}u_{yy} + u_{xx}u_{zz} + u_{yy}u_{zz}) + (C_{11} - C_{12})(u_{xy}^2 + u_{xz}^2 + u_{yz}^2), \tag{2}$$

where u_{ij} are components of the strain tensor; C_{11} and

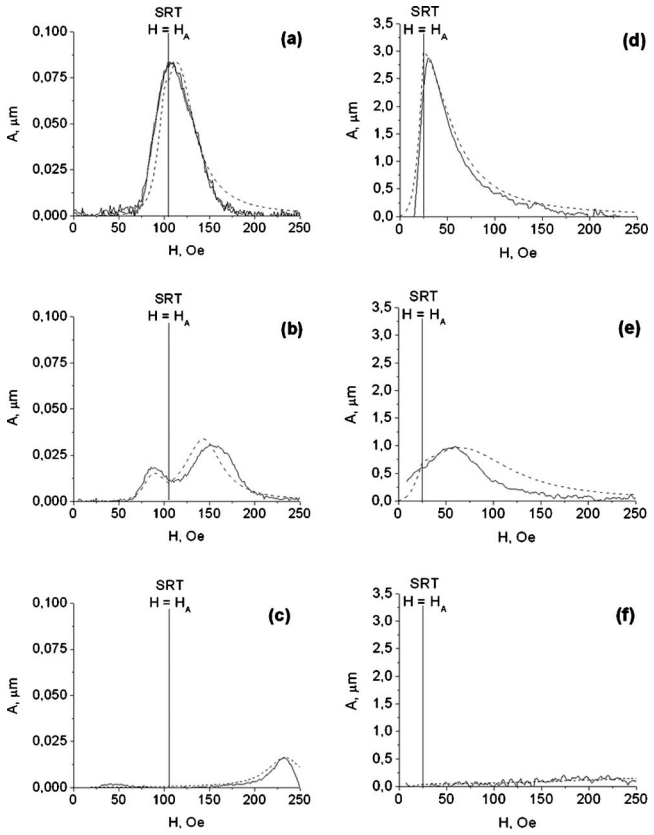

FIG. 3. Magnetic field dependence of the amplitude of sample vibrations at different FMR frequencies for $La_{0.7}Sr_{0.3}MnO_3$ film [(a)—814 MHz, (b)—1183 MHz, (c)—1760 MHz)] and for $TbCo_2$/FeCo nanostructure [(d)—1172 MHz, (e)—2174 MHz, (f)—4918 MHz)]: solid line-experiment, dashed line-theory.

C_{12}—the elastic stiffness constants. In this expression, the difference between elastic moduli of the substrate and the film was neglected.

The magnetic part of energy volume density consists of the Zeeman energy, the anisotropy energy and the energy of demagnetization field.

$$F_m = -(\vec{M}\vec{H}) + \frac{H_{A0}}{2M_0}|(\vec{M}\times\vec{n})|^2 + \frac{1}{2}\vec{M}\hat{N}\vec{M} \tag{3}$$

with: $\vec{n}$—the unit vector that is collinear to the easy axis of the sample (Fig. 4); H_{A0}—the effective value of anisotropy field; $\vec{M}$—the magnetic moment. $\hat{N}$ is the demagnetizating tensor, which is assumed to be the same as for an infinite plate. Thus it has just only one nonzero element $N_{zz}=4\pi$.

The magnetoelastic energy volume density is defined by the magnetostrictive term in isotropic model

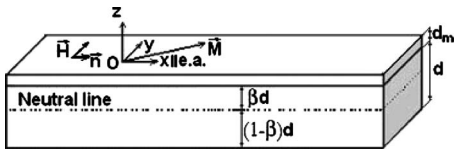

FIG. 4. Geometry of the system: e.a.—easy axis, M—magnetization of the magnetic film, d_m and d—thicknesses of the magnetic film and substrate, respectively, β parameter defining the position of the neutral line, H—external magnetic field.

$$F_{me}^V = b^{\gamma,2}\{[(M_x/M_0)^2 - 1/3]u_{xx} + [(M_y/M_0)^2 - 1/3]u_{yy} + [(M_z/M_0)^2 - 1/3]u_{zz} + 2/M_0^2[M_xM_yu_{xy} + M_yM_zu_{yz} + M_xM_zu_{xz}]\}. \tag{4}$$

Here $b^{\gamma,2}$ is the magnetoelastic constant.

The magnetization can be subdivided into three parts such as: static, HF, and LF:

$$M_i(t) = M_i^0 + m_i(t) + \mu_i(t). \tag{5}$$

Elastic deformations contain static and LF dynamic parts.

$$\hat{u}(t) = \hat{u}_0 + \hat{\varepsilon}(t). \tag{6}$$

HF part of elastic strains is assumed to be negligibly small because of relatively thick substrate and the high value of HF mechanical absorption in the sample.

To obtain the energy of the flexural vibrations we can introduce the vertical displacement $U=u_z$. In this case the dynamic part of the deformations is defined by the second derivatives of the displacement:$\varepsilon_{ij}=-(z-z_0)\partial^2U/\partial x_i\partial x_j$, where i,j are equal to 1 or 2, and $\varepsilon_{zz}=-(C_{12}/C_{11})(\varepsilon_{xx}+\varepsilon_{yy})$. Here z_0 is the position of the neutral section.

It can be shown[22] that Lagrangian of the system after integration by z may be expressed via kinetic and potential components of the surface energy density

$$L = \int_S dS\{1/2\rho_S\dot{U}^2(x,y,t) - F_e^S[\hat{U}(x,y,t)] - F_{me}^S[\vec{M},\hat{U}(x,y,t)]\} \tag{7}$$

Taking into account presentation (5) one can obtain the following expressions for elastic and magnetoelastic potential energy parts related to the LF excitations:

$$F_e^S = 1/2\hat{e}\hat{U}^2(x,y,t) = \frac{d^3}{3}(3\beta^2-3\beta+1)(C_{11}-C_{12})\left[\frac{1}{2}\left(1+\frac{C_{12}}{C_{11}}\right)(\Delta U)^2 + \left(\frac{\partial^2U}{\partial x\,\partial y}\right)^2 - \frac{\partial^2U}{\partial x^2}\frac{\partial^2U}{\partial y^2}\right], \tag{8}$$

$$F_{me}^S(t) = \frac{\beta d d_m b^{\gamma,2}}{M_0^2}\left[\frac{\partial^2U}{\partial x^2}\left(-2M_x^0\mu_x(t) - \overline{\left\{[m_x(t)]^2 - [m_z^2(t)]\frac{C_{12}}{C_{11}}\right\}^\tau}\right) - \frac{\partial^2U}{\partial y^2}\left(-2M_y^0\mu_y(t) - \overline{\left((m_y(t))^2 - (m_z^2(t))\frac{C_{12}}{C_{11}}\right)^\tau}\right) - \frac{\partial^2U}{\partial x\,\partial y}(M_x^0\mu_y(t) + M_y^0\mu_x(t) + \overline{m_x(t)m_y(t)}^\tau)\right]. \tag{9}$$

The averaging in Eq. (9) is made over the time period τ, which is much higher than the period of HF oscillations of magnetization but much smaller than the period of LF vibrations.

One can expand overall elastic deformation into normal vibration modes

$$U(x,y,t) = \sum_n U_n(x,y)A_n(t). \tag{10}$$

Substituting this expansion in Eqs. (7)–(9) one can write the Lagrangian of a mode n:

$$L_n = 1/2M_n\dot{A}_n^2 - 1/2k_nA_n^2 + F_n(t)A_n, \tag{11}$$

where the following notations are used:

$$\begin{cases} M_n = \int_S dS\rho_S U_n^2, \\ k_n = \int_S dS\hat{e}\hat{U}_n^2, \\ F_n(t) = \int_S dSF_{me}^S(\vec{M},\hat{U}_n). \end{cases} \tag{12}$$

Equation of motion for $A_n(t)$ can be derived from Lagrange's differential equation:

$$\frac{\partial}{\partial t}\frac{\partial L_n}{\partial \dot{A}_n} - \frac{\partial L_n}{\partial A_n} + \frac{\partial D}{\partial \dot{A}_n} = 0 \tag{13}$$

Here we used Rayleigh dissipation function in the form:[23] $D=\delta_n M_n\dot{A}_n^2$.

Hence we can obtain the equation of motion for amplitude $A_n(t)$ of a mode "n" in the form of an oscillator equation:

$$M_n(\ddot{A}_n + 2\delta_n\dot{A}_n + \Omega_n^2 A_n) = F_n(t). \tag{14}$$

Here Ω_n is the resonance frequency of the mode $\Omega_n = (\kappa_n/M_n)^{1/2}$.

Following Eqs. (12) and (14), one can obtain the Fourier amplitude of elastic vibrations that is proportional to the LF magnetization and to the averaged value of the square of the HF magnetization components.

$$A_n(\Omega) = \frac{\eta_n\beta d_m d b^{\gamma,2}}{M_n\sqrt{(\Omega^2-\Omega_n^2)^2+(2\delta_n\Omega)^2}}\frac{1}{T}\int_{-T/2}^{T/2} dte^{-i\Omega t} \times\left[\overline{m_x^2(t) - m_z^2(t)\frac{C_{12}{}^{\tau}}{C_{11}}} + 2M_{0x}\mu_x(t)\right]/M_0^2. \tag{15}$$

Here $\eta_n = \int \partial^2 U_n/\partial x^2 dS$, $T=2\pi/\Omega_n$, *and* Ω is a frequency divisible by Ω_n

Positions of the neutral lines defined by β are different for the static and dynamic resonance cases.[22] In the static case, the neutral line defined by the parameter β has the position minimizing the sum of elastic and magnetoelastic energies: $\beta=2/3$. For the dynamic case, the vibration modes have an antisymmetrical distribution of deformations relatively to the mean section of the cantilever and, therefore: $\beta=1/2$. The explicit form of the function $U_n(x)$ is given in the Appendix A.

It could be derived from Eqs. (15) and (B.1) that the amplitude of elastic vibrations of the fundamental flexural mode at resonance frequency is equal to

$$A_n(\Omega_n) = 0.231b^{\gamma,2}\Gamma\frac{1}{T}\int_{-T/2}^{T/2} dte^{-i\Omega t}\left[\overline{m_x^2(t) - m_z^2(t)\frac{C_{12}{}^{\tau}}{C_{11}}} + 2M_{0x}\mu_x(t)\right]/M_0^2. \tag{16}$$

Here Γ is a parameter, which is composed of the geometric and acoustic properties of the sample: $\Gamma = d_m/\rho_S c_s\delta_n$, where c_S is the longitudinal sound velocity in the sample and ρ_S is the surface density of the structure. The Eq. (16) together with the results of calculations of $m_x(t)$ and $\mu_x(t)$ are used to obtain the magnetic field dependence of the vibration amplitudes presented in Fig. 3.

Calculations of the components of magnetization are carried out using the Landau–Lifshitz equation:

$$\frac{\partial\vec{M}}{\partial t} = -\gamma[\vec{M}\times\vec{H}_{eff}] + \frac{\alpha}{M_0}\left[\vec{M}\times\frac{\partial\vec{M}}{\partial t}\right] \tag{17}$$

where α is the coefficient of magnetic relaxation and $\vec{H}_{eff}$ is the effective magnetic field.

$$\vec{H}_{eff} = -\frac{\partial F}{\partial\vec{M}}. \tag{18}$$

According to presentation (5) of the magnetic moment, the effective magnetic field is divided in static, LF and HF components:

$$\vec{H}_{eff} = \vec{H}_{eff}^0 + \vec{h}_{eff}^{\Omega}(t) + \vec{h}_{eff}^{\omega}(t), \tag{19}$$

where superscripts Ω and ω correspond to LF and HF parts, respectively. The equilibrium ground state of the magnetic system is given by the static equation:

$$[\vec{M}_0\times\vec{H}_0^{eff}] = 0. \tag{20}$$

According to Eqs. (3), (4), and (18), one can obtain the components of the static effective field

$$\vec{H}_{eff}^0 = \begin{pmatrix} 0 \\ -H + \frac{H_A}{M_0}M_y^0 \\ \frac{H_A}{M_0}M_z^0 + 4\pi M_z^0 \end{pmatrix}. \tag{21}$$

In the definition of the value H_A that corresponds to the SRT bias field we took into account the contribution of the static magnetostrictive strains. Generally the static strain contains two parts. One of them is created during the preparation of the films and corresponds to the direction of magnetization parallel to the easy axis in the nonstressed structure. This part contributes to the anisotropy field in Eq. (3) with value $H_{me}=2(b^{\gamma,2})^2/M_0(C_{11}-C_{12})$. It is included in definition of H_A in Eq. (21): $H_A=H_{A0}+H_{me}$. The second component of the static strain follows variations in the equilibrium direction of $\vec{M}_0$. These deformations are proportional to the ratio of the film and the substrate thicknesses $(d_m/d)\sim 10^{(-3)\div(-4)}$ and introduce a negligibly small contribution in H_{eff}^0.

The HF component of the effective magnetic field can be deduced from Eq. (17) as

$$h^{\omega}_{eff}(t) = h_i(t) + S^{ij} m_j(t), \tag{22}$$

where: $S^{ij} = \partial (H^0_{eff})_j / M_i$.

Using Eq. (5), one can describe HF magnetization dynamics in a linear approximation of the Landau–Lifshitz Eq. (17)

$$\frac{\partial \vec{m}}{\partial t} = -\gamma \left[\vec{M}_0 \times \left(\frac{H^0_{eff}}{M_0} \vec{m}(t) - \vec{h}^{\omega}_{eff}(t) - \frac{\alpha}{\gamma M_0} \frac{\partial \vec{m}}{\partial t} \right) \right] \tag{23}$$

The solution of Eq. (23) is expressed via the magnetic susceptibility tensor: $\vec{m}(t) = \hat{\chi}(\omega)\vec{h}(t)$. The explicit form of $\hat{\chi}(\omega)$ is presented in the Appendix B.

LF dynamics of magnetization is described by the second-order nonlinear part of the Landau–Lifshitz equation

$$\frac{\partial \vec{\mu}}{\partial t} = -\gamma \left\{ \vec{M}_0 \times \left[\frac{H^0_{eff}}{M_0} \vec{\mu}(t) - \vec{h}^{\Omega}_{eff}(t) - \frac{\alpha_{\Omega}}{\gamma M_0} \frac{\partial \vec{\mu}}{\partial t} \right] \right\} - \gamma \overline{[\vec{m} \times \vec{h}^{\omega}_{eff}]}^{\tau}, \tag{24}$$

where α_{Ω} is LF magnetic relaxation coefficient. The LF part of the effective field (19) is equal to:

$$h^{\Omega}_{eff}(t) = S^{ij} \mu_j + S^{ilj} \overline{m_l m_j}^{\tau}, \tag{25}$$

where $S^{ilj} = \partial^2 (H^0_{eff})_j / \partial M_i \partial M_l$

As it was mentioned above the nonlinear alternative terms are averaged for the time period τ: $1/\Omega \gg \tau \gg 1/\omega$. In the expression (25) we neglected by elastomagnetic feedback effect caused by the LF deformations and proportional to the ratio d_m/d.

Following Eqs. (24) and (25) one can obtain the LF part of the magnetization:

$$\mu_i(t) = \kappa_{ikl} \overline{h_k(t) h_l(t)}^{\tau} \tag{26}$$

where:

$$\kappa_{ikl} = -4\Theta_{ij} (\varepsilon_{jmk} \chi'_{ml} + \varepsilon_{juv} S^{\nu v} (\chi'_{uk} \chi'_{vl} + \chi''_{uk} \chi''_{vl})) / (\pi \det \hat{\Theta}). \tag{27}$$

Here: ε_{ijk} is the Levi–Civita symbol; χ'_{vl} and χ''_{vl} are real and imaginary components of the HF magnetic susceptibility, respectively; $\hat{\Theta} = \hat{A}(\Omega)$ is the operator of the linear Landau–Lifshitz equation for LF vibrations, which differs from the high frequency operator by the LF Ω instead of HF ω (see Appendix B).

The analyze of the matrix $\chi(\omega)$ [see Eq. (B.1)] shows that the FMR line for uniaxial magnetic film has two maxima near SRT: one for saturation ($H > H_A$) and another for angular phases ($H < H_A$) that are caused by χ'' and κ_{ikl} maximas. In the case of the $TbCo_2$/FeCo nanostructure only one resonance peak was observed in all the involved frequency range. That is explained by the strong attenuation of HF spin excitations in rare earth compounds. On contrary, the curves for the perovskite film have two resonant peaks in most part of frequency range except the area near SRT where the HF relaxation increases. The best fitting of calculations with the experimental data in the case of the perovskite film was obtained for relative HF magnetic attenuation factors equal to $\alpha_A = 0.605$ for 1172 MHz, $\alpha_{B,C} = 0.355$ for 1172 MHz and for 2174 MHz, which are almost twice lower than for the $TbCo_2$/FeCo nanostructure: $\alpha_A = 0.925$ for 1172 MHz, $\alpha_B = 0.575$ for 2174 MHz, and $\alpha_C = 0.275$ for 4918 MHz. In the area which is sufficiently far from SRT the relative HF magnetic attenuation factors decrease slowly. This fact seems to be caused by the domain structure that appears in the vicinity of SRT.[11]

According to the calculations using Eqs. (16), (26), and (B.1), the increase in amplitude of the LF vibrations excited by the HF electromagnetic field in FMR conditions near SRT is clear. The behavior of the curves for the vibration amplitude presented in Fig. 3 is similar to the behavior of FMR curves presented in Fig. 2. One can see that the mechanical response for the $TbCo_2$/FeCo nanostructure is greater in order of magnitude than for the perovskite film. The comparison of the multipliers Γ in Eq. (19) gives the ratio: $\Gamma_{LSMO}/\Gamma_{TbCo_2/FeCo} \approx 1.126$. This data, together with the magnetostriction coefficient ratio $b^{\gamma,2}_{LSMO}/b^{\gamma,2}_{TbCo_2/FeCo} \approx 0.1$, explain the favorable mechanical response of the $TbCo_2$/FeCo structure in spite of the higher HF attenuation relative to the one in the $La_{0.7}Sr_{0.3}MnO_4$ sample.

IV. CONCLUSION

The experimental and theoretical data on FMR and magnetoelastic demodulation in the $TbCo_2$/FeCo nanostructure and $La_{0.7}Sr_{0.3}MnO_4$ thin film, deposited on Si and $NdGaO_3$ cantilevers, respectively, show that LF vibrations of the cantilever can be amplified when FMR is excited by HF electromagnetic field near SRT. The experiments have been carried out at high frequencies from below 1 to above 4 GHz. Rare earth manganitestrontium perovskites demonstrated clear resonance properties in the majority of the high frequency range. At the same time, it is shown that the $TbCo_2$/FeCo nanostructure has a much higher mechanical response in spite of the higher HF attenuation. This is caused by the fact that the $TbCo_2$/FeCo nanostructure has a high value of magnetoelastic coupling factor. The results of the calculations are in good agreement with the experimental data of measurements of the FMR line and with the data of the optical detection of elastic vibrations of the magnetostrictive cantilever under HF electromagnetic field. The phenomenon under consideration can find various applications in the field of MMMS controlled by a HF electromagnetic field.

ACKNOWLEDGMENTS

We thank Dr. G. A. Ovsyannikov for providing perovskite samples and discussions. This work was supported by RFBR under Grants Nos. 09-02-93107-NCNIL_a and 08-02-00785-a, the ANR under Project No. ANR-08-NAN O-035-01, and by the French Embassy in Moscow (French Ministry of Foreign Affairs).

APPENDIX A

According to the elasticity theory[22] one dimensional displacement $U_n(x)$ in flexural modes is:

$$U_n(x) = [\cos(\eta_n l) + ch(\eta_n l)][\cos(\eta_n x) - ch(\eta_n x)] + [\sin(\eta_n l) - sh(\eta_n l)][\sin(\eta_n x) - sh(\eta_n x)]. \quad \text{(A.1)}$$

Here $\eta_n = \sqrt[4]{\Omega_n^2(\mathrm{P}/c_S^2 I_y)}$, l—the length of sample, P—the sample cross-section, $c_S = \sqrt{(1/\rho)(C_{11} - C_{12})(1 + (C_{12}/C_{11}))}$ is the longitudinal sound velocity, ρ is the material density, I_y—moment of inertia along $0y$ axis.

APPENDIX B

$$\hat{\chi}^{(n)} = \frac{1}{detA}\begin{pmatrix} A_{31}M_y^0 & -A_{31}M_x^0 & -A_{11}M_y^0 + A_{21}M_x^0 \\ A_{32}M_y^0 & -A_{32}M_x^0 & -A_{12}M_y^0 + A_{22}M_x^0 \\ A_{33}M_y^0 & -A_{33}M_x^0 & -A_{13}M_y^0 + A_{23}M_x^0 \end{pmatrix}. \quad \text{(B.1)}$$

Here A_{ij}—an algebraical complement to ij-element of matrix A:

$$\hat{A}(n\Omega + \omega) = \begin{pmatrix} \frac{i(n\Omega + \omega)}{\gamma} & 0 & a_{13} \\ 0 & \frac{i(n\Omega + \omega)}{\gamma} & a_{23} \\ a_{31} & a_{32} & \frac{i(n\Omega + \omega)}{\gamma} \end{pmatrix}. \quad \text{(B.2)}$$

The elements of matrix A are:

$$\begin{cases} a_{13} = H + 4\pi M_y^0, \\ a_{31} = -H + M_y^0 \dfrac{H_A}{M_0}, \\ a_{23} = -M_x^0\left(\dfrac{H_A}{M_0} + 4\pi\right), \\ a_{32} = M_x^0 \dfrac{H_A}{M_0} \end{cases} . \quad \text{(B.3)}$$

[1] J. B. Youssef, N. Tiercelin, F. Petit, H. Le Gall, V. Preobrazhensky, and P. Pernod, IEEE Trans. Magn. **38**, 2817 (2002).
[2] N. Tiercelin, J. B. Youssef, V. Preobrazhensky, P. Pernod, and H. L. Gall, J. Magn. Magn. Mater. **249**, 519 (2002).
[3] H. Le Gall, J. Ben Youssef, F. Socha, N. Tiercelin, V. Preobrazhensky, and P. Pernod, J. Appl. Phys. **87**, 5783 (2000).
[4] N. Tiercelin, P. Pernod, V. Preobrazhensky, H. Le Gall, J. Ben Youssef, P. Mounaix, and D. Lippens, Sens. Actuators **81**, 162 (2000).
[5] E. Quandt and H. Holleck, Microsyst. Technol. **1**, 178 (1995).
[6] E. Quandt, J. Alloys Compd. **258**, 126 (1997).
[7] N. Tiercelin, P. Pernod, V. Preobrazhensky, H. Le Gall, and J. Ben Youssef, Ultrasonics **38**, 64 (2000).
[8] V. I. Ozhogin and V. Preobrazhensky, J. Magn. Magn. Mater. **100**, 544 (1991).
[9] Y. V. Gulyaev, I. E. Dikstein, and V. G. Shavrov, Phys. Usp. **167**, 7 (1997).
[10] V. D. Buchel'nikov, N. K. Dan'shin, L. T. Tsymbal, and V. G. Shavrov, Phys. Usp. **39**, 547 (1996).
[11] A. Klimov, N. Tiercelin, V. Preobrazhensky, and P. Pernod, IEEE Trans. Magn. **42**, 3090 (2006).
[12] N. Tiercelin, V. Preobrazhensky, P. Pernod, H. Le Gall, and J. Ben Youssef, J. Magn. Magn. Mater. **210**, 302 (2000).
[13] N. Tiercelin, V. Preobrazhensky, P. Pernod, and A. Ostachenko, Appl. Phys. Lett. **92**, 062904 (2008).
[14] N. Tiercelin, A. Talbi, V. Preobrazhensky, P. Pernod, V. Mortet, K. Haenen, and A. Soltani, Appl. Phys. Lett. **93**, 162902 (2008).
[15] N. Tiercelin, V. Preobrazhensky, V. Mortet, A. Talbi, A. Soltani, K. Haenen, and P. Pernod, J. Magn. Magn. Mater. **321**, 1803 (2009).
[16] L. I. Koroleva, R. V. Demin, A. M. Balbashov, Pis'ma Zh. Eksp. Teor. Fiz. **65**, 449 (1997).
[17] R. V. Demin, L. I. Koroleva, and A. M. Balbashov, J. Magn. Magn. Mater. **177–181**, 871 (1998).
[18] H. Boschker, M. Mathews, E. P. Houwman, H. Nishikava, A. Vailionis, G. Koster, G. Rijners, and D. H. A. Blank, Phys. Rev. B **79**, 214425 (2009).
[19] G. A. Ovsyannikov, A. M. Petrzhik, I. V. Borisenko, A. A. Klimov, Y. A. Ignatov, V. V. Demidov, and S. A. Nikitov, Zh. Eksp. Teor. Fiz. **108**, 56 (2009).
[20] C. Kittel, Phys. Rev. **110**, 836 (1958).
[21] A. I. Ahieser, V. G. Bar'yahtar, and S. V. Peletminskiy, *Spin Waves* (Nauka, Moscow, 1967).
[22] L. D. Landau and E. M. Lifshitz, *Theory of Elasticity*, 1st ed. (Pergamon, London, 1959).
[23] B. J. Torby, *Advanced Dynamics for Engineers* (Holt, Rinehart, and Winston, New York, 1984).